



Synthesis and Direct Comparison of the Anticancer Activities of Phomopsolides D/E and Two 7-Oxa-/7-Aza-analogues

Journal:	<i>MedChemComm</i>
Manuscript ID	MD-RES-02-2019-000121.R1
Article Type:	Research Article
Date Submitted by the Author:	24-Apr-2019
Complete List of Authors:	Aljahdali, Alhanouf; Northeastern University, Chemistry Freedman, Seth; Northeastern University, Chemistry Scott, Jana; University of Minnesota Twin Cities Campus, Chemistry Li, Miaosheng; West Virginia University, Chemistry O'Doherty, George; Northeastern University, Chemistry

Synthesis and Direct Comparison of the Anticancer Activities of Phomopsolides D/E and Two 7-Oxa-/7-Aza-analogues

Received 00th January 20xx,
Accepted 00th January 20xx

Alhanouf Z. Aljahdali,^{a†} Seth A. Freedman,^{a†} Jana Scott,^{b†} Miaosheng Li^{c*} and George A. O'Doherty^{a*}

DOI: 10.1039/x0xx00000x

www.rsc.org/

The synthesis of two stable phomopsolide natural products (D and E) and two analogues are presented. The cytotoxicity of these four compounds is surveyed and compared across a panel of NCI-cancer cell lines. This analysis found moderate cytotoxicities (2–50 μM) for the majority of the cell lines with phomopsolide D being more active than phomopsolide E and the 7-oxa analogue being commensurately more active than the 7-aza analogue.

The phomopsolide class of polyketide natural products is made up of five 6-substituted 5,6-dihydro-5-hydroxypyran-2-ones that are all acylated with a tiglate ester group at the 5-position (Fig. 1).^{1,2} The structural variation in the class of natural products exist in the *n*-pentyl side chain at the 6-position (Fig. 1). The structural range of the known phomopsolides A–E consist of having or not having a C-6/7 alkene in *E*- or *Z*-configuration and oxidation in either the alcohol or ketone stage at C-8. All known phomopsolides have an (*S*)-configured alcohol at the C-9 position. The initial discovery of the phomopsolides by Grove¹ and Stierle² was a result of a program aimed at finding antiboring/antifeeding natural products that would prevent the elm bark beetle (*Hylurgopinus rufipes*) from spreading fungus (*Ophiostoma ulmi*) associated with Dutch elm disease.^{3,4} The five phomopsolides were also found to exhibit antimicrobial activity (e.g., *S. aureus*).⁵

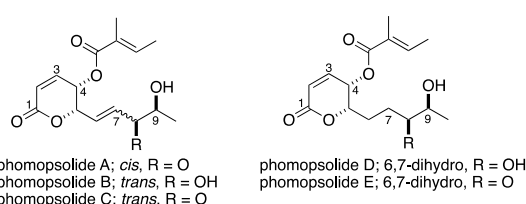


Figure 1: The phomopsolide natural products (A–E)

As a result of their unique structure and biological activity, the phomopsolides have garnered a fair amount of attention from the synthetic community. This interest has resulted in a total of seven successful syntheses of the phomopsolide natural products. In addition, there have been several syntheses of related analogues. The first synthesis was by Noshita in 1994 and was of phomopsolide B.⁶ Synthetic interest in the phomopsolides returned the following century, with our syntheses of phomopsolide C and phomopsolide D, in 2002 and 2004 respectively.^{7,8} This was followed up the following year with a synthesis of phomopsolide C by Blechert.⁹ Over the subsequent decade, other reports appeared detailing the syntheses of phomopsolide C by Prasad¹⁰ and Yadav,¹¹ as well as, a synthesis of the C-4,5-bisepimer of phomopsolide by Atmakur.¹² Most recently, we reported a synthesis of phomopsolide E, which built upon our *de novo* approach to phomopsolide D.¹³ Over this same time period we have also investigated the synthesis of phomopsolide stereoisomers and congeners, such as 7-oxa-phomopsolide E,¹⁴ 7-aza-phomopsolide E¹⁵ and related C-4/C-5 stereoisomers.^{8,13,14,15}

^a Dept. of Chemistry and Chem. Bio., Northeastern Univ. Boston, MA 02115.

^b Dept. of Chemistry, Univ. of Minnesota, Minneapolis, MN 55455.

^c Dept. of Chemistry, West Virginia Univ. Morgantown, WV 26506.

† Co-First Authors the order is alphabetical.

Electronic Supplementary Information (ESI) available: [details of any supplementary information available should be included here]. See DOI: 10.1039/x0xx00000x

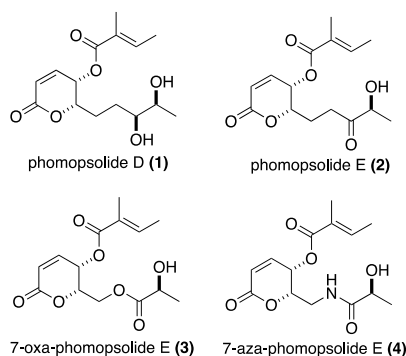
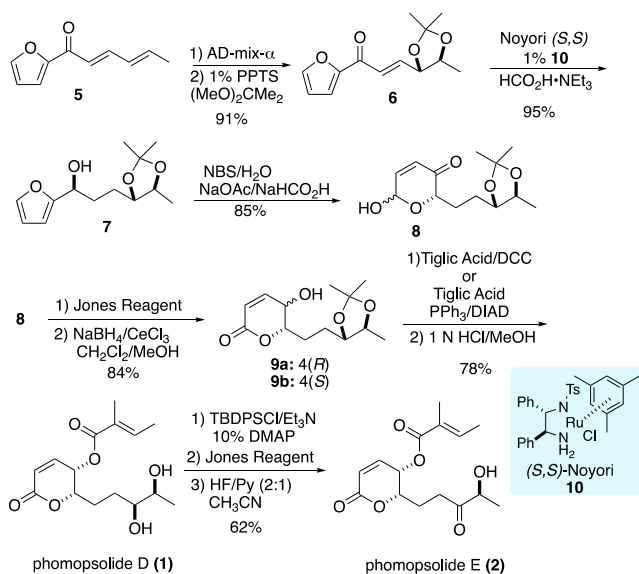


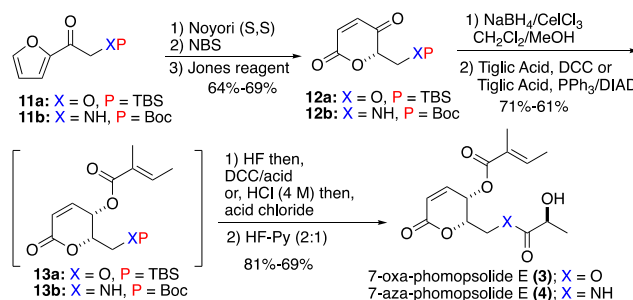
Figure 2: Phomopsolide D and E and their congeners

Over the years, we have been developing various *de novo* asymmetric approaches to polyketide natural products,¹⁶ with an emphasis on those that contain pyranone rings.¹⁷ Our interest in the phomopsolides came as part of a larger ongoing effort to study the structure activity relationship (SAR) of natural products, with a particular focus on stereochemistry (S-SAR). These SAR/S-SAR studies have covered a wide range of structural motifs (*e.g.*, polyketides,¹⁸ as well as a range of carbohydrates¹⁹) and biological activities (*e.g.*, anticancer, antibacterial, antiviral and related protein targets). In this regard, our efforts towards the phomopsolides was part of a long-term effort aimed at providing material for a systematic study of their SAR. These practical realities caused us to focus on phomopsolides D and E, due to an instability we found with the C-6/7 alkene. Herein we give the full account of our efficient syntheses of two phomopsolide natural products (D and E) and two analogue natural products (7-oxa and 7-aza). In addition, we detail, for the first time, our use of a comprehensive cancer cell cytotoxicity screen to comparatively evaluate the validity of the 7-oxa- and 7-aza-substitution.

Scheme 1: *De novo* syntheses toward phomopsolide D (1) and phomopsolide E (2)

The syntheses of phomopsolide D and E that we finally settled on is outlined in (Scheme 1). The route is a *de novo*

asymmetric route, as it derives the absolute and relative stereochemistry in two catalytic asymmetric reactions. The first being a Sharpless dihydroxylation of diene 5 and the second being a reagent Noyori reduction of acylfuran 6. Specifically, a two-step oxidation/protection converted dienone 5 into acylfuran 6, which can be diastereoselectively reduced to form furan alcohol 7 with excellent stereocontrol and yield. An Achmatowicz oxidation/hydration/rearrangement was used to convert furyl alcohol 7 into 8-hydroxypyranone 8. A subsequent two-step Jones oxidation and Luche reduction reaction sequence was used to convert 8 in to a 2:1 mixture of pyranones 9a/b (75%). A combination of retentive (tiglic acid/DCC, 82%) and invertive (tiglic acid PPh₃/DEAD) ester formations converts the mixture of diastereomer into acetonide protected natural product, which was easily deprotected to form phomopsolide D (HCl(aq), 95%). Then in a three-step sequence phomopsolide D was selectively oxidized to give phomopsolide E. This began with the selective protection of the diol at the C-8 position with a TBDPS group.²⁰ A Jones oxidation was then used to oxidize the resulting alcohol into ketone, which could be deprotected with HF/Py to give the natural product phomopsolide E (2) (62% yield in 3 steps)



Scheme 2: Syntheses of 7-Oxa-phomopsolide E (3) and 7-Aza-phomopsolide E (4)

We next turned to the synthesis of the 7-oxa- and 7-aza-phomopsolide analogues 3 and 4 (Scheme 2). The synthesis began with the suitably protected oxa- and aza-substituted acylfurans 11a and 11b, with a TBS and Boc protecting group, respectively. Both acylfurans 11a/b were asymmetrically reduced under the Noyori conditions, oxidatively rearranged under the Achmatowicz conditions and oxidized with the Jones reagent to give enediones 12a/b. Luche reduction of the enediones 12a/b gave a mixture of diastereomers, which were separated and acylated in a retentive (tiglic acid/DCC) and invertive (tiglic acid PPh₃/DEAD) fashion to give esters 13a/b. Finally, a three step deprotection, acylation and deprotection sequence on 13a/b gave the two desired analogue targets, 7-oxa-phomopsolide E (3) and 7-aza-phomopsolide E (4).

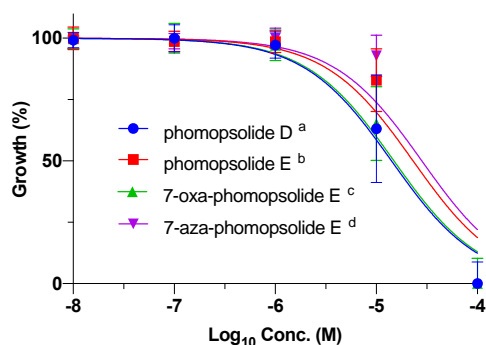


Figure 3 Average phomopsolide (**1-4**) cytotoxicity curves against the NCI cell lines. ^a Data for 53 out of the 60 cell lines are presented, ^b Data for 57 out of the 60 cell lines are presented, ^c Data for 58 out of the 60 cell lines are presented, ^d Data for 38 out of the 60 cell lines are presented

With the synthesis of the four phomopsolides (**1-4**) in hand, we next turned to their evaluation for cytotoxicity against the NCI 60 cell line panel from 10 μM to 100 μM .^{21,22} The cell lines used are maintained by the Developmental Therapeutics Program at the National Cancer Institute (For information regarding the cell lines see: <https://dtp.cancer.gov>).²³ In general, compounds (**1-4**) demonstrated good cytotoxicity against the whole class of cell lines with IC_{50} ranging from a low of 2 μM to a high of 49 μM . The average data for the four phomopsolides across the full 60 cell line panels is plotted in Fig. 3 and outlined in Table 1. Not all the IC_{50} S-curves suitably flattened out at 10 μM , which negatively effects the accuracy of the IC_{50} calculations. As a result, the data from these experiments were excluded from this analysis. This phenomenon is more likely to occur for the less cytotoxic compound, such as 7-aza-phomopsolide E (**4**), for which only 38 of the 60 cell lines gave data that could be included (Fig. 3/Table 1). The other, more active, phomopsolides (**1-3**) had interpretable data giving IC_{50} values in 53, 57 and 58 of the 60 cell lines tested, respectively.

Table 1 IC_{50} for NCI cell lines

Compound	Average IC_{50}	IC_{50} Range
phomopsolide D ^a	14 μM	$\pm 14 \mu\text{M}$
phomopsolide E ^b	23 μM	$\pm 16 \mu\text{M}$
7-oxa-phomopsolide E ^c	15 μM	$\pm 10 \mu\text{M}$
7-aza-phomopsolide E ^d	28 μM	$\pm 18 \mu\text{M}$

^a Data for 53 out of the 60 cell lines are presented, ^b Data for 57 out of the 60 cell lines are presented, ^c Data for 58 out of the 60 cell lines are presented, ^d Data for 38 out of the 60 cell lines are presented.

Some general observations can be drawn from the pan-cell line average data, such as: 1) phomopsolide D ($\text{IC}_{50} = 14 \mu\text{M}$) was in general more active than phomopsolide E ($\text{IC}_{50} = 23 \mu\text{M}$); 2) phomopsolide D and 7-oxa-phomopsolide E ($\text{IC}_{50} = 15 \mu\text{M}$) were the most similar in terms of cytotoxic and the most cytotoxic; whereas, 4) the 7-aza phomopsolide E ($\text{IC}_{50} = 28 \mu\text{M}$) exhibited the least cytotoxicity and was most similar to phomopsolide E. This analysis, of course, is limited by the fact

that there is significant variation across the panel of 60 cell lines, as evident by the large and overlapping range of IC_{50} values for compounds **1-4**. To try to control for these variations, we looked at the average IC_{50} values of compounds **1-4** for the nine different tissue types in the panel (*cf.*, Figs. 4-12/Tables 2-10). This analysis more precisely shows (less overlapping range of IC_{50}) the same overall trend of compounds **1** and **3** being more similar and active and compounds **1** and **3** being more similar and less active.

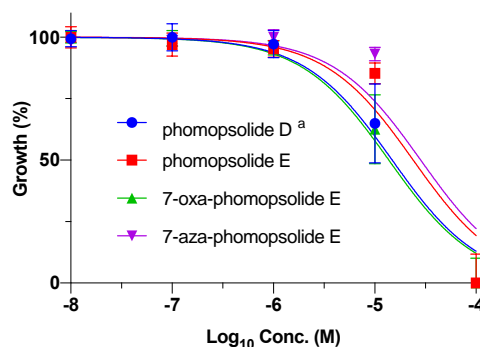


Figure 4 Average phomopsolide (**1-4**) cytotoxicity curves against melanoma cancer cell lines (LOX IMVI, MALME-3M, M14, SK-MEL-2, SK-MEL-28, SK-MEL-5, UACC-257, and UACC-62) against the \log_{10} concentration of the compound introduced to the cells. ^a Data for 7 out of the 8 cell lines are presented.

When the cytotoxicities for the phomopsolides (**1-4**) are plotted for only the eight melanoma cell lines (*i.e.*, LOX IMVI, MALME-3M, M14, SK-MEL-2, SK-MEL-28, SK-MEL-5, UACC-257, and UACC-62), very similar activities and trend were seen (Fig. 4/Table 2), albeit with smaller non-overlapping variation. The trends for the average data against the melanoma cell lines showed very similar trends, such as: 1) phomopsolide D ($\text{IC}_{50} = 15 \mu\text{M}$) and 7-oxa-phomopsolide E ($\text{IC}_{50} = 13 \mu\text{M}$) were the most active and possessed very similar activity; whereas, 2) phomopsolide E ($\text{IC}_{50} = 24 \mu\text{M}$) and 7-aza-phomopsolide E ($\text{IC}_{50} = 28 \mu\text{M}$) were the least active and similar in terms of cytotoxicity.

Table 2 IC_{50} melanoma cancer cell lines

Compound	Average IC_{50}	IC_{50} Range
phomopsolide D ^a	15 μM	$\pm 4 \mu\text{M}$
phomopsolide E	24 μM	$\pm 7 \mu\text{M}$
7-oxa-phomopsolide E	13 μM	$\pm 3 \mu\text{M}$
7-aza-phomopsolide E	28 μM	$\pm 9 \mu\text{M}$

^a Data for 7 out of the 8 cell lines are presented.

When the cytotoxicities for the phomopsolides (**1-4**) are plotted against the six CNS cancer cell lines (*i.e.*, SF-268, SF-295, SF-539, SNB-19, SNB-75, and U251), the average activities and relative trend were similar (Fig. 5/Table 3) with only slightly overlapping IC_{50} ranges, such as: 1) phomopsolide D ($\text{IC}_{50} = 17 \mu\text{M}$) and 7-oxa-phomopsolide E ($\text{IC}_{50} = 16 \mu\text{M}$) were the most active and possessed very similar activity; whereas, 2) phomopsolide E ($\text{IC}_{50} = 26 \mu\text{M}$) and 7-aza-phomopsolide E

($IC_{50} = 29 \mu\text{M}$) were the least active and similar in terms of cytotoxicity.

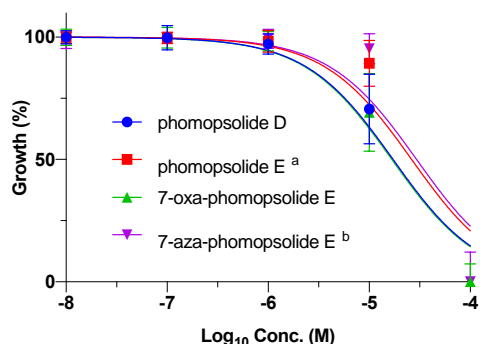


Figure 5 Average phomopsolide (1-4) cytotoxicity curves against CNS cancer cell lines (SF-268, SF-295, SF-539, SNB-19, SNB-75, and U251), excluding outliers, against the \log_{10} concentration of the compound introduced to the cells. ^a Data for 5 out of the 6 cell lines are presented. ^a Data for 4 out of the 6 cell lines are presented.

Table 3 IC_{50} CNS cancer cell lines

Compound	Average IC_{50}	IC_{50} Range
phomopsolide D	17 μM	$\pm 5 \mu\text{M}$
phomopsolide E ^a	26 μM	$\pm 11 \mu\text{M}$
7-oxa-phomopsolide E	16 μM	$\pm 5 \mu\text{M}$
7-aza-phomopsolide E ^b	29 μM	$\pm 15 \mu\text{M}$

^a Data for 5 out of the 6 cell lines are presented. ^b Data for 4 out of the 6 cell lines are presented.

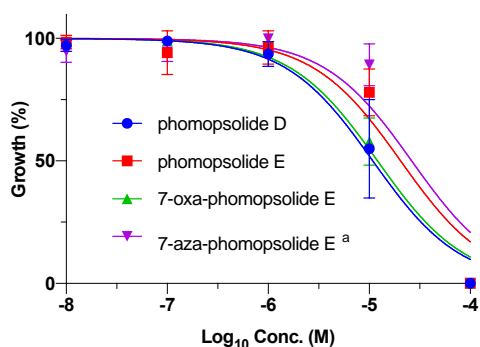


Figure 6 Average phomopsolide (1-4) cytotoxicity curves against breast cancer cell lines (MCF7, NCI/ADR-RES, MDA-MB-231/ATCC, HS 578T, MDA-MB-435, and T-47D) against the \log_{10} concentration of the compound introduced to the cells. ^a Data for 3 out of the 4 cell lines are presented.

When the cytotoxicities for the phomopsolides (1-4) are plotted against the six breast cancer cell lines (*i.e.*, MCF7, NCI/ADR-RES, MDA-MB-231/ATCC, HS 578T, MDA-MB-435, and T-47D), the average activities and relative trend were similar with only slightly overlapping IC_{50} ranges (Fig. 6/Table 4), such as: 1) phomopsolide D ($IC_{50} = 11 \mu\text{M}$) and 7-oxa-phomopsolide E ($IC_{50} = 12 \mu\text{M}$) were the most active and possessed very similar activity; whereas, 2) phomopsolide E ($IC_{50} = 20 \mu\text{M}$) and 7-aza-phomopsolide E ($IC_{50} = 26 \mu\text{M}$) were the least active and similar in terms of cytotoxicity.

Table 4 IC_{50} breast cancer cell lines

Compound	Average IC_{50}	IC_{50} Range
phomopsolide D	11 μM	$\pm 3 \mu\text{M}$
phomopsolide E	20 μM	$\pm 6 \mu\text{M}$
7-oxa-phomopsolide E	12 μM	$\pm 2 \mu\text{M}$
7-aza-phomopsolide E ^a	26 μM	$\pm 10 \mu\text{M}$

^a Data for 3 out of the 4 cell lines are presented.

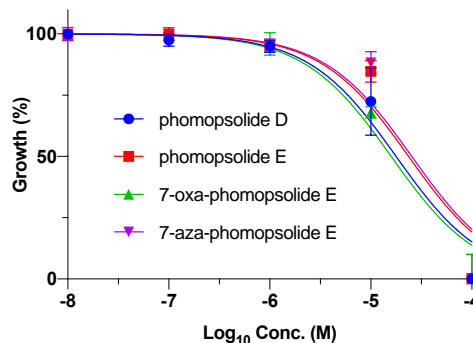


Figure 7 Average phomopsolide (1-4) cytotoxicity curves against prostate cancer cell (PC-3 and DU-145), against the \log_{10} concentration of the compound introduced to the cells.

When the cytotoxicities for the phomopsolides (1-4) are plotted against the two prostate cancer cell lines (*i.e.*, PC-3 and DU-145), the average activities and relative trend were similar, however with much more overlapping IC_{50} values (Fig. 7/Table 5). Once again, the greatest cytotoxicities were seen for phomopsolide D ($IC_{50} = 18 \mu\text{M}$) and 7-oxa-phomopsolide E ($IC_{50} = 16 \mu\text{M}$); whereas, 2) phomopsolide E ($IC_{50} = 23 \mu\text{M}$) and 7-aza-phomopsolide E ($IC_{50} = 25 \mu\text{M}$) were the least active and similar in terms of cytotoxicity.

Table 5 IC_{50} prostate cancer cell lines

Compound	Average IC_{50}	IC_{50} Range
phomopsolide D	18 μM	$\pm 9 \mu\text{M}$
phomopsolide E	23 μM	$\pm 15 \mu\text{M}$
7-oxa-phomopsolide E	16 μM	$\pm 7 \mu\text{M}$
7-aza-phomopsolide E	25 μM	$\pm 18 \mu\text{M}$

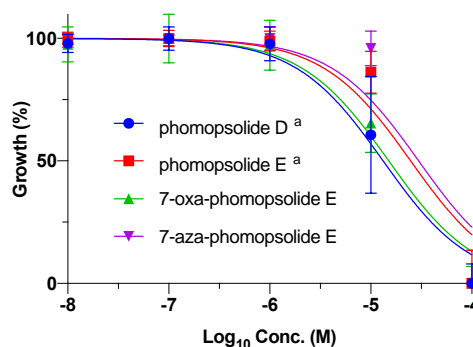


Figure 8 Average phomopsolide (1-4) cytotoxicity curves against renal cancer cell lines (786-O, A498, ACHN, CAKI-1, RXF 393, SN12C, TK-10 and UO-31) against the \log_{10}

concentration of the compound introduced to the cells. ^a Data for 7 out of the 8 cell lines are presented.

When the cytotoxicities for the phomopsolides (**1-4**) are plotted against the eight renal cancer cell lines (*i.e.*, 786-0, A498, ACHN, CAKI-1, RXF 393, SN12C, TK-10 and UO-31), the average activities and relative trend were similar with only slightly overlapping IC₅₀ ranges (Fig. 8/Table 6), such as: 1) phomopsolide D (IC₅₀ = 13 μM) and 7-oxa-phomopsolide E (IC₅₀ = 15 μM) were the most active and possessed very similar activity; whereas, 2) phomopsolide E (IC₅₀ = 25 μM) and 7-aza-phomopsolide E (IC₅₀ = 30 μM) were the least active and similar in terms of cytotoxicity.

Table 6 IC₅₀ renal cancer cell lines

Compound	Average IC ₅₀	IC ₅₀ Range
phomopsolide D ^a	13 μM	± 4 μM
phomopsolide E ^a	25 μM	± 8 μM
7-oxa-phomopsolide E	15 μM	± 4 μM
7-aza-phomopsolide E	30 μM	± 11 μM

^a Data for 7 out of the 8 cell lines are presented.

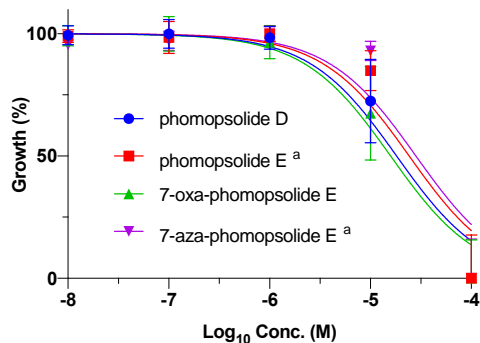


Figure 9 Average phomopsolide (**1-4**) cytotoxicity curves against ovarian cancer cell lines (IGROV1, OVCAR-3, OVCAR-4, OVCAR-5, OVCAR-8 and SK-OV-3) against the log₁₀ concentration of the compound introduced to the cells. ^a Data for 4 out of the 6 cell lines are presented.

When the cytotoxicities for the phomopsolides (**1-4**) are plotted against the six ovarian cancer cell lines (*i.e.*, IGROV1, OVCAR-3, OVCAR-4, OVCAR-5, OVCAR-8 and SK-OV-3), the average activities and relative trend were similar, albeit with overlapping IC₅₀ ranges (Fig. 9/Table 7). Phomopsolide D (IC₅₀ = 18 μM) and 7-oxa-phomopsolide E (IC₅₀ = 16 μM) were again the most active and phomopsolide E (IC₅₀ = 24 μM) and 7-aza-phomopsolide E (IC₅₀ = 28 μM) were similar in terms of cytotoxicity and again the least active.

Table 7 IC₅₀ ovarian cancer cell lines

Compound	Average IC ₅₀	IC ₅₀ Range
phomopsolide D	18 μM	± 6 μM
phomopsolide E ^a	24 μM	± 10 μM
7-oxa-phomopsolide E	16 μM	± 6 μM
7-aza-phomopsolide E ^a	28 μM	± 14 μM

^a Data for 4 out of the 6 cell lines are presented.

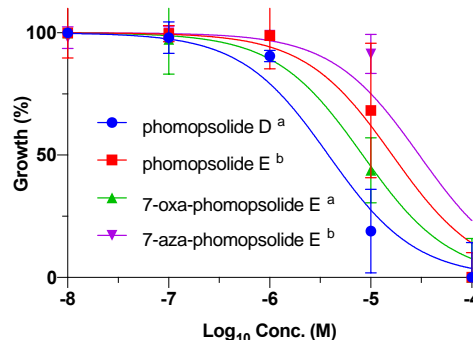


Figure 10 Average phomopsolide (**1-4**) cytotoxicity curves against leukemia cancer cell lines (CCRF-CEM, HL-60(TB), K-562, MOLT-4, and RPMI-8226) against the log₁₀ concentration of the compound introduced to the cells. ^a Data for 2 out of the 5 cell lines are presented. ^b Data for 4 out of the 5 cell lines are presented.

Of the NCI cancer cell lines, the leukemia cell lines showed the greatest sensitivity to the most active phomopsolide, compound **1**, with an IC₅₀ of 4 μM. When the cytotoxicities for the phomopsolides (**1-4**) are plotted against the five leukemia cancer cell lines (*i.e.*, CCRF-CEM, HL-60(TB), K-562, MOLT-4, and RPMI-8226), the average activities and relative trend were similar, with only slightly overlapping ranges of IC₅₀ (Fig. 10/Table 8). For instance, phomopsolide D (IC₅₀ = 4 μM) and 7-oxa-phomopsolide E (IC₅₀ = 8 μM) were the most active and very similar in activity; whereas, 2) phomopsolide E (IC₅₀ = 16 μM) and 7-aza-phomopsolide E (IC₅₀ = 30 μM) were similar in activity and the least cytotoxic.

Table 8 IC₅₀ Leukemia cancer cell lines

Compound	IC ₅₀ (μM)	IC ₅₀ Range
phomopsolide D ^a	4 μM	± 3 μM
phomopsolide E ^b	16 μM	± 9 μM
7-oxa-phomopsolide E ^a	8 μM	± 5 μM
7-aza-phomopsolide E ^b	30 μM	± 14 μM

^a Data for 2 out of the 5 cell lines are presented. ^b Data for 4 out of the 5 cell lines are presented.

When the cytotoxicities for the phomopsolides (**1-4**) are plotted against the eight non-small cell lung cancer cell lines (*i.e.*, A549/ATCC, EKVX, HOP-62, NCI-H226, NCI-H23, NCI-H322M, NCI-H460, and NCI-H522), the average activities and relative trend were similar with only slightly overlapping IC₅₀ range, (Fig. 11/Table 9), such as: 1) phomopsolide D (IC₅₀ = 18 μM) and 7-oxa-phomopsolide E (IC₅₀ = 19 μM) were the most active and possessed very similar activity; whereas, 2) phomopsolide E (IC₅₀ = 26 μM) and 7-aza-phomopsolide E (IC₅₀ = 27 μM) were the least active and similar in terms of cytotoxicity.

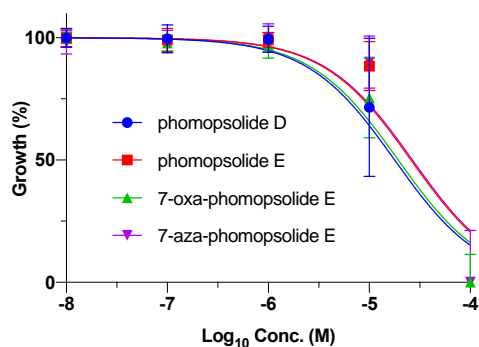


Figure 11 Average phomopsolide (1-4) cytotoxicity curves against non-small cell lung cancer cell lines (A549/ATCC, EKVX, HOP-62, NCI-H226, NCI-H23, NCI-H322M, NCI-H460, and NCI-H522), against the \log_{10} concentration of the compound introduced to the cells.

Table 9 IC_{50} non-small cell lung cancer cell lines

Compound	Average IC_{50}	IC_{50} Range
phomopsolide D	18 μ M	\pm 6 μ M
phomopsolide E	26 μ M	\pm 8 μ M
7-oxa-phomopsolide E	19 μ M	\pm 5 μ M
7-aza-phomopsolide E	27 μ M	\pm 9 μ M

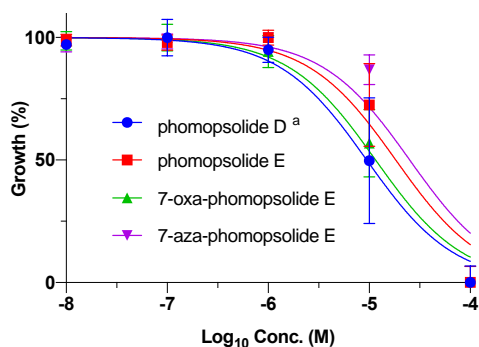


Figure 12 Average phomopsolide (1-4) cytotoxicity curves against colon cancer cell lines (COLO 205, HCC-2998, HCT-116, HCT-15, HT29, KM12, and SW-620) against the \log_{10} concentration of the compound introduced to the cells. ^a Data for 6 out of the 7 cell lines are presented.

Finally, when the cytotoxicities for the phomopsolides (1-4) are plotted against the seven colon cancer cell lines (*i.e.* COLO 205, HCC-2998, HCT-116, HCT-15, HT29, KM12, and SW-620), the average activities and relative trend were similar and the range of cytotoxicities were small (Fig. 12/Table 10). Phomopsolide D (IC_{50} = 9 μ M) and 7-oxa-phomopsolide E (IC_{50} = 11 μ M) were again the most active and very similar in activity. Once again, phomopsolide E (IC_{50} = 18 μ M) and 7-aza-phomopsolide E (IC_{50} = 25 μ M) were the least active and similar in terms of cytotoxicity.

Table 10 IC_{50} for Colon cancer cell lines

Compound	Average IC_{50}	IC_{50} Range
phomopsolide D ^a	9 μ M	\pm 3 μ M
phomopsolide E	18 μ M	\pm 5 μ M
7-oxa-phomopsolide E	11 μ M	\pm 3 μ M
7-aza-phomopsolide E	25 μ M	\pm 8 μ M

^a Data for 6 out of the 7 cell lines are presented.

Conclusions

In conclusion, the synthesis of two phomopsolide natural products and two related analogues was achieved, and subsequently analyzed for cytotoxicity across a panel of NCI-cancer cell lines. The data suggests that there is comparable biological activity in all four phomopsolides. Phomopsolide D and 7-oxo-phomopsolide E present the most cytotoxicity with nearly identical activity in most of the cancer cell types, with phomopsolide E and 7-aza-phomopsolide E being consistently less active.

Acknowledgements

The authors gratefully acknowledge the National Science Foundation (CHE-1565788) and the National Institutes of Health (AI144196-01 and AI142040) for their support of this work. AZA would like to thank King Abdullah Scholarship Program for a fellowship. SAF would like to thank the Northeastern University Office of Undergraduate Research and Fellowships for the Undergraduate Research and Creative Endeavor Award.

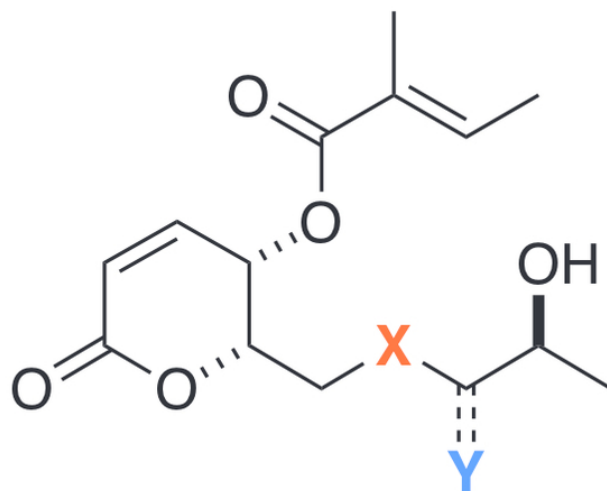
Conflicts of interest

There are no conflicts to declare.

Notes and references

- 1 J. F. Grove, *J. Chem. Soc., Perkin Trans.* 1985, **1**, 865-869.
- 2 D. B. Stierle, A. A. Stierle and B. Ganser, *J. Nat. Prod.* 1997, **60**, 1207-1209.
- 3 H. Becker, *Agricultural Research* 1996, **44**, 4-8.
- 4 F. S. Santamour and S. E. Bentz, *J. of Arboriculture* 1995, **21**, 122-131.
- 5 T. Noshita, T. Sugiyama, K. Yamashita, and T. Oritani, *Biosci. Biotech. Biochem.*, 1994, **58**, 740.
- 6 T. Noshita, T. Sugiyama, K. Yamashita and T. Oritani, *Biosci. Biotech. Biochem.* 1994, **58**, 740-744.

- 7 J. M. Harris and G. A. O'Doherty, *Tetrahedron Lett.* 2002, **43**, 8195-8199.
- 8 M. Li, and G. A. O'Doherty, *Tetrahedron Lett.* 2004, **45**, 6407-6411.
- 9 S. Michaelis and S. Blechert, *Org. Lett.* 2005, **7**, 5513-5516.
- 10 K. R. Prasad and P. Gutala, *Tetrahedron* 2012, **68**, 7489-7493.
- 11 D. V. Reddy, G. Sabitha and J. S. Yadav, *Tetrahedron Lett.* 2015, **56**, 4112-4114.
- 12 N. R. Emmadi, C. Bingi, C. G. Kumar, P. Yedla and K. Atmakur, *Synthesis* 2014, **46**, 2945-2950.
- 13 J. M. Harris, M. Li and G. A. O'Doherty, *Heterocycles*, **99**, ASAP. DOI: 10.3987/COM-18-S(F)96
- 14 M. Li, J. G. Scott and G. A. O'Doherty, *Tetrahedron Lett.* 2004, **45**, 1005-1009.
- 15 A. Z. Aljahdali, S. A. Freedman, M. Li, and G. A. O'Doherty, *Tetrahedron*, 2018, **74**, 7121-7126.
- 16 (a) C. M. Goins, T. D. Sudasinghe, X. Liu, Y. Wang, G. A. O'Doherty, and D. R. Ronning, *Biochemistry*, 2018, **57**, 2383; (b) X. Liu, Y. Wang, R. I. Duclos, and G. A. O'Doherty, *ACS Med. Chem. Lett.*, 2018, **9**, 274; (c) X. Liu, Y. Wang, and G. A. O'Doherty, *Asian J. Org. Chem.*, 2015, **4**, 994; (d) M. Mulzer, B. Tiegs, Y. Wang, G. W. Coates, and G. A. O'Doherty, *J. Am. Chem. Soc.*, 2014, **136**, 10814.
- 17 (a) T. J. Hunter, Y. Wang, J. Zheng, and G. A. O'Doherty, *Synthesis* 2016, **48**, 1700; (b) M. F. Cuccarese, Y. Wang, P. J. Beuning, and G. A. O'Doherty, *ACS Med. Chem. Lett.* 2014, **5**, 522; (c) Y. Wang, and G. A. O'Doherty, *J. Am. Chem. Soc.* 2013, **135**, 9334; (d) T. J. Hunter, and G. A. O'Doherty, *G. A. Org. Lett.* 2001, **3**, 2777; (e) C. M. Smith, and G. A. O'Doherty, *Org. Lett.* 2003, **5**, 1959.
- 18 (a) J. M. Harris and G. A. O'Doherty *Org. Lett.*, 2000, **2**, 2983; (b) J. M. Harris and G. A. O'Doherty *Tetrahedron*, 2000, **57**, 5161.
- 19 (a) M. Li, Y. Li, K. A. Ludwik, Z. M. Sandusky, D. A. Lannigan and G. A. O'Doherty, *Org. Lett.* 2017, **19**, 2410-2413. (b) K. A. Ludwik, J. P. Campbell, M. Li, L. Li, Z. M Sandusky, L. Pasic, M. E. Sowder, D. R Brenin, J. A. Pietenpol, G. A. O'Doherty and D. A. Lannigan, *Mol. Cancer Ther.* 2016, **15**, 2598-2608. (c) S. O. Bajaj, P. Shi, P. J. Beuning and G. A. O'Doherty, *Med. Chem. Commun.*, 2014, **5**, 1138-1142. (d) H. Cai, H.-Y. L. Wang, R. Venkatadri, D.-X. Fu, M. Forman, S. O. Bajaj, H. Li, G. A. O'Doherty and R. Arav-Boger, *ACS Med. Chem. Lett.* 2014, **5**, 395-399. (e) J. W. Hinds, S. B. McKenna, E. U. Sharif, H.-Y. L. Wang, N. G. Akhmedov and G. A. O'Doherty, *ChemMedChem*. 2013, **8**, 63-69. (f) P. Shi, M. Silva, B. Wu, H.-Y. L. Wang, N. G. Akhmedov, M. Li, P. Beuning and G. A. O'Doherty, *ACS Med. Chem. Lett.* 2012, **3**, 1086-1090.
- 20 G. Pedrocchi-Fantoni and S. Servi, *J. Chem. Research (S)*, 1986, **6**, 199.
- 21 (a) M. C. Alley, D. A. Scudiero, P. A. Monks, M. L. Hursey, M. J. Czerwinski, D. L. Fine, B.J. Abbott, J. G. Mayo, R. H. Shoemaker, and M. R. Boyd, *Cancer Research* 1988, **48**, 589-601. (b) M. R. Grever, S. A. Schepartz, and B. A. Chabner, The National Cancer Institute: Cancer Drug Discovery and Development Program. Seminars in Oncology, 1992, **19**, 622-638. (c) M. R. Boyd, and K. D. Paull, *Drug Development Research* 1995, **34**, 91-109. (d) R. H. Shoemaker, *Nature Reviews*, 2006, **6**, 813-823.
- 22 (a) X. Yu, G. A. O'Doherty, *Org. Lett.* 2008, **10**, 4529-4532. (b) A. Iyer, M. Zhou, N. Azad, H. Elbaz, L. Wang, D. K. Rogalsky, Y. Rojanasakul, G. A. O'Doherty and J. M. Langenhan, *ACS Med. Chem. Lett.* 2010, **1**, 326-330.
- 23 R. H. Shoemaker *Nature Rev Cancer* **2006**, **6**, 813-823.



phomopsolide D: **X** = CH₂, **Y** = H/OH
phomopsolide E: **X** = CH₂, **Y** = O
7-oxa-phomopsolide E: **X** = O, **Y** = O
7-aza-phomopsolide E: **X** = NH, **Y** = O

75x58mm (300 x 300 DPI)